RAA 2021 Vol. **21** No. **11**, 276(7pp) doi: 10.1088/1674-4527/21/11/276

http://www.raa-journal.org *http://iopscience.iop.org/raa*

Research in Astronomy and Astrophysics

First investigation of eclipsing binary KIC 9026766: analysis of light curve and periodic changes

Somaye Soomandar and Abbas Abedi

Faculty of Sciences, University of Birjand, Iran; *S.soomandar@birjand.ac.ir*

Received 2021 June 16; accepted 2021 August 9

Abstract We investigate a short-period W UMa binary KIC 9026766 with an orbital period of 0.2721278 d in the Kepler field of view. By applying an automated q-search for the folded light curve and producing a synthetic light curve for this object based on the PHOEBE code, we calculate the fundamental stellar parameters. We also analyze the $O-C$ curve of the primary minima. The orbital period changes can be attributed to the combination of an upward quadratic function and light-travel time effect (LTTE) due to a possible third body with a minimum mass of $0.029\,M_{\odot}$ and an orbital period of 972.5866 ± 0.0041 d. The relative luminosity of the primary and secondary eclipses (Min I − Min II) is calculated. The periodogram of the residuals of the LTTE and Min I − Min II show peaks with the same period of 0.8566 d. The background effect of two nearby stars on our target is the possible reason for this signal. By considering the amplitudes and periods of the remaining signals in the $O-C$ curve of minima, spot motion is possible.

Key words: techniques: photometric — stars: individual: KIC 9026766

1 INTRODUCTION

The role of eclipsing binary (EB) stars is very important in stellar astrophysics. Properties such as the mass, radius and luminosity of these stars can be calculated with an accuracy of less than 1 percent (Pietrzyński et al. 2019) and the existing stellar evolution models can be modified using these parameters (Torres et al. 2014). EB stars contain two stars in which the components orbit around their common barycenter (i.e., their orbit results in eclipses), and most of our knowledge about their characteristics comes from this motion. One of the reliable measures to determine the parameters of the components is the variations in the $O-C$ curve of minima. Physical factors such as mass transfer (Pribulla et al. 2000), apsidal motion (Guinan & Maloney 1985), Applegate effect (Applegate 1992), Shklovskii effect (Shklovskii 1970), Barycentric and Asymmetric Transverse Velocities (BATV) (Conroy et al. 2018), light-travel time effect (LTTE, Borkovits & Hegedüs 1996) and dynamical effects of a third body on the binary orbit can be the reasons for variations in the $O-C$ curve.

In addition to these effects, the observed erratic variations may indicate unidentified apparent timing effects (Borkovits et al. 2015). Furthermore, stellar spots can cause spurious $O-C$ curve variations, which are thoroughly investigated in Tran et al. (2013) and Balaji et al. (2015).

KIC 9026766 is a contact binary in the Kepler field of view, and one of its flags in the EB Catalog (Abdul-Masih et al. 2016)[1] is TM that indicates multiple bodies in the system. Therefore, we analyze the $O-C$ curve to investigate the triple-body effect of the binary. Moreover, the light curve is modeled.

2 OBSERVATIONS

KIC 9026766 was observed by the Kepler satellite during quarters 0–17 in long-cadence (LC) mode with effective integration times of 30 min. No light curve has been reported for this target in short-cadence (SC) mode (Abdul-Masih et al. 2016). Some parameters are presented in the Kepler EB Catalog, such as the morphology parameter which was introduced by Matijevič et al. (2012) as an identifier to determine the type of binary that has the value between 0 and 1, where 0 indicates a completely detached binary, and 1 indicates a contact binary. Moreover, the effective temperature (accurate to 200 K) of the target is estimated utilizing ground-based optical multi-

[1] http://keplerebs.villanova.edu/

Table 1 Observation Specifications of KIC 9026766

Parameter	Value in Catalog
Kepler ID	9026766
2MASS ID	J19341881 + 4518354
RA	19 34 18.816
Dec	+ 45 18 35.46
Kepler mag.	14.998 ± 0.02
$T_{\rm eff}(K)$	4888 ± 2.0
$\log(g)$	4.7 ± 0.5
Period (d)	$0.2721278 \pm 2E-7$
$\rm BJD_0$	$2454964.846798 \pm 0.015238$
Morphology	0.76

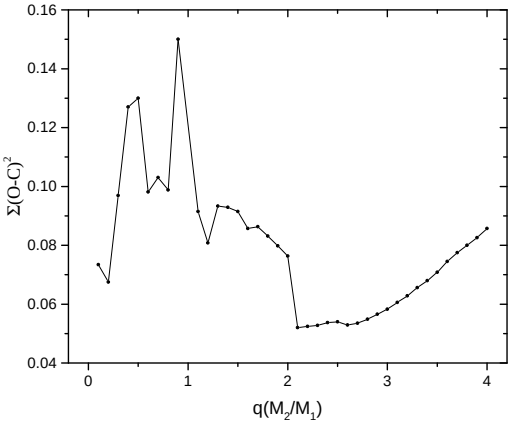

Fig. 1 Automated q-search in the range [0.1–4.00].

color photometry of the Two Micron All Sky Survey (2MASS) (Skrutskie et al. 2006). Other observational parameters such as surface gravity $\log g$ (accurate to 0.5 dex), Barycentric Julian Date of the primary eclipse $\rm BJD_0$ (accurate to 0.015238) and the period of the binary (accurate to 0.0000002 d) are presented in Tabel 1. The nearby stars Gaia DR2 2127972818460821504 and Gaia DR2 212 7972818467257344 are located within 0.5 and 1.0 arcsec of the target[2] respectively. Since each pixel is 4 arcsec across, blending of sources is expected. We checked the pixel data using the Lightkurve Python package (Lightkurve Collaboration 2018) for each quarter of the chosen target pixel files in the aperture; Abdul-Masih et al. (2016) was selected as the best pixel data for this system, so we relied on the detrended light curves in the Kepler EB Catalog.

3 LIGHT CURVE SOLUTION

To find the initial guess of the orbital parameters of KIC 9026766, we performed an automated q-search in the same way as done by Soomandar & Abedi (2020). The

[2] http://cdsportal.u-strasbg.fr/?target=KIC209026766

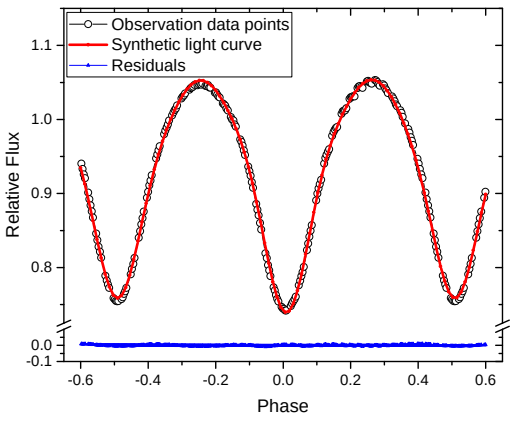

Fig. 2 Light curve solution of KIC 9026766. Observational data points (*blank circles*), synthetic light curve (*solid red line*) and residuals (*blue triangles*).

Wilson-Devinney code was imported as a subroutine to Matlab, and the least squares method was employed to obtain the initial guess of the parameters.

One cycle of the light curve in LC mode has almost 14 data points. For the light curve solution, we used 4.08 days of data points and phase-binned them. The morphology parameter of this target was reported as 0.78, so we chose mode 3 (contact not in thermal equilibrium) in the Wilson-Devinney code. The fixed parameters were as follows: effective temperature $T_1 = T_{\rm eff}$, bolometric albedos $A_1 = A_2 = 0.5$ (Rucinski 1969) and gravity brightening $g_1 = g_2 = 0.32$ (Lucy 1967). Moreover, we chose the linear regime of van Hamme (1993) for limb darkening coefficients and considered two reflection effects. For q, the iteration was considered within the range [0.1–4.00] with 0.1 steps; for the temperature of the secondary component, we iterated within [4000–7000] K with steps of 1000 K and the stellar gravitational potential parameter $\Omega_1 = \Omega_2$ was iterated in the range $[\Omega(L_1) - \Omega(L_2)]$ with steps of 0.05. The minimum indicates that $\Sigma(O-C)^2$ for q=2.1, and the corresponding curve is plotted in Figure 1. The Prša et al. (2011)[3] catalog lists the principal parameters determined by a neural network analysis of the phased light curves. One of the computed parameters of contact systems is the photometric mass ratio, and our result for $q = 2.1$ is close to what they have calculated, $q = 2.09477$. Therefore, we chose this value for the light curve solution.

In the following, we use the PHOEBE Legacy (SVN 2012–07–08) by selecting mean Kepler passband and applying finite integration time for LC mode. We repeated the fitting by considering the differential correction

[3] http://keplerebs.villanova.edu/v2

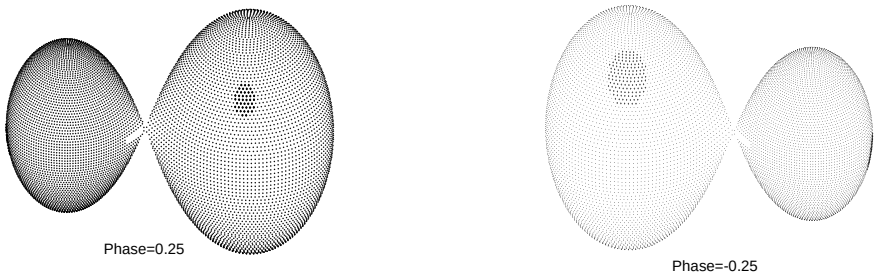

Fig. 3 Three-dimensional view of KIC 9026766 at phases –0.25 and 0.25.

method, and we used the following five free parameters: the temperature of the second star, T_2, orbital inclination, i, stellar surface gravitational potential, $\Omega_1 = \Omega_2$, the monochromatic luminosity of the primary star, L_1, and q. Then, we added cool spots characterized by radius, temperature, co-latitude and latitude on the surface of the two components to obtain the best solution. The final parameters are tabulated in Table 2. Figure 2 shows the synthetic light curve and Figure 3 displays the three-dimensional model of the system.

To calculate the mass of the components of KIC 9026766, we assume that the more massive component is a normal main sequence star and its mass could be estimated as $M_2 = 0.73\,M_\odot$, corresponding to the spectral type K2 (Cox 2000). By relying on the mass ratio q and M_2 values, the mass of the primary component is calculated as $M_1 = 0.35\,M_\odot$.

4 MEASURING MINIMA

The observed minima were calculated by fitting a Lorentzian function to the individual minima in the same way as done by Soomandar & Abedi (2020). To find the initial parameters of the Lorentzian function, we used the maximum and minimum relative flux and mean Barycentric Julian Date for an individual eclipse. We also used the Scipy.curve-fit package of Python to minimize $\Sigma(O-C)^2$ and calculated the observational eclipse times.

The linear ephemeris of this target is reported on the website `http://keplerebs.villanova.edu` as follows

$$T_{\min,1} = 2454964.8467981(\pm 0.015238) + 0.2721278(\pm 0.0000002)E\,. \quad (1)$$

Here E is the observational epoch. We used Equation (1) to calculate the $O-C$ curves of the primary and secondary minima of eclipses. The $O-C$ curves of minima are plotted in Figure 4.

Table 2 Orbital Parameters of Light Curve Solution for KIC 9026766

Parameter	Value
$A_1 = A_2^a$	0.5
$g_1 = g_2^a$	0.32
T_1^a	4880
T_2	4757 ± 0.411
q	2.077 ± 0.0068
i^0	69.42 ± 0.04
$\Omega_{1,2}$	5.3591 ± 0.0006
$\frac{L_1}{L_1+L_2}$	0.3692 ± 0.0041
f	0.2 percent
x_1^a	0.66025
x_2^a	0.66699
r_1(pole)	0.2961 ± 0.084
r_2(pole)	0.4174 ± 0.008
r_1(side)	0.3098 ± 0.099
r_2(side)	0.4447 ± 0.105
r_1(back)	0.34243 ± 0.153
r_2(back)	0.47142 ± 0.136
Spot co-latitude^b	100.01 ± 0.015
Spot longitude^b	181.20 ± 0.02
Spot radius^b	12.01 ± 0.02
$(\frac{T_{\rm spot}}{T_{\rm surf}})^b$	0.9 ± 0.02
Spot co-latitude^c	45.01 ± 0.025
Spot longitude^b	271.20 ± 0.02
Spot radius^b	15.2 ± 0.1
$(\frac{T_{\rm spot}}{T_{\rm surf}})^c$	0.95 ± 0.02
Spot co-latitude^c	55.01 ± 0.023
Spot longitude^b	90.0 ± 0.03
Spot radius^b	8.1 ± 0.1
$(\frac{T_{\rm spot}}{T_{\rm surf}})^c$	0.8 ± 0.02
$\Sigma(O-C)^2$	0.0321

^{a}: Fixed Parameter; ^{b}: Primary Star; ^{c}: Secondary Star.

Conroy et al. (2014) calculated the precise eclipse times for 1279 close binaries in the Kepler EB Catalog. To compare the result of this work to the calculated $O-C$ curve by Conroy et al. (2014), we downloaded the $O-C$ curve of primary minima for this target and compared the periodogram of their results with the periodogram of primary minima of this work. The resulting curve is displayed in the Figure 5.

Table 3 Coefficients of Quadratic Fit

A	B	C
$0.00224 \pm 2.35724 \times 10^{-5}$	$-1.35557 \times 10^{-}6 \pm 1.96721 \times 10^{-8}$	$2.42862 \times 10^{-10} \pm 3.54376 \times 10^{-12}$

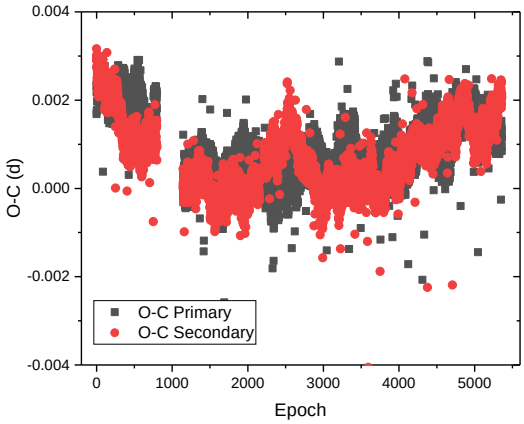

Fig. 4 $O-C$ curves of minima of KIC 9026766. The primary and secondary minima of eclipses are represented by *black squares* and *red circles*, respectively.

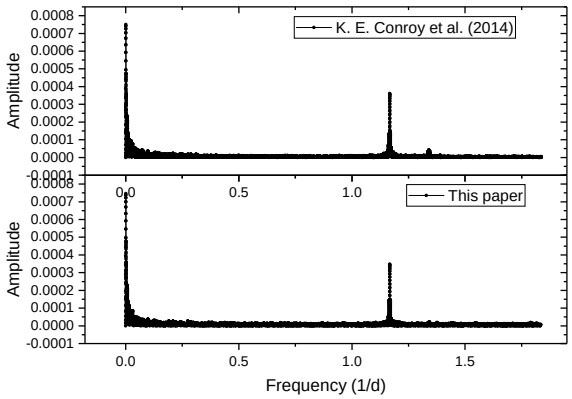

Fig. 5 *Top panel*: The periodogram analysis of the $O-C$ curve from Conroy et al. (2014). *Bottom panel*: The periodogram analysis of the $O-C$ curve from this work.

5 ORBITAL PERIOD CHANGES

To investigate the orbital changes over time, we considered the $O-C$ curve of the primary minima. Fitting a quadratic function to the $O-C$ curve of minima exhibits an increase in the period; the corresponding plot is featured in the left panel of Figure 6 and the fitting coefficients are listed in Table 3.

The rate of period increase is calculated by Equation (2) (Hilditch 2001).

$$\dot{P} = \frac{2C}{P_{orb}} = \frac{2 \times 2.42862 \times 10^{-10}}{0.2721278} = 1.784911 \times 10^{-9} \pm 7.08752 \times 10^{-12} \mathrm{d\ yr^{-1}}\,. \quad (2)$$

By considering mass conservation, the mass exchange rate can be calculated utilizing Equation (3).

$$\frac{\dot{P}}{P} = -3\frac{\dot{M}_2(M_1 - M_2)}{M_1 M_2} = 1.4700 \times 10^{-9} \pm 0.5837 \times 10^{-11} M_\odot \mathrm{yr}^{-1}\,, \quad (3)$$

where the positive sign indicates that the direction of mass transfer is from the less massive component to the more massive one.

The residuals of the quadratic fit manifest periodic changes over time, so we consider the LTTE as possibly signaling the presence of a third body.

In the following, we apply the periodogram analysis by using Period04 (Lenz & Breger 2005) for the residuals of the quadratic fit. The strong peak shows a period of almost 972 d for the third body. The LTTE term is given in Equation (4) (Irwin 1952).

$$(O-C)_{LTTE} = \frac{A}{\sqrt{1 - e^2\cos^2(\omega)}} \times \left(\frac{1-e^2}{1 + e\cos(\nu)}\sin(\nu+\omega) + e\sin(\omega)\right), \quad (4)$$

where $A = \frac{a_{1,2}\sin(i)}{c}\sqrt{1 - e^2\cos^2(\omega)}$ and $a_{1,2}$ is the semi-major axis of the relative orbit of the eclipsing system around the center of mass (in au), i is the inclination of the third-body orbit, e is the eccentricity of the third-body orbit, ω is the longitude of periastron and ν is the true anomaly. The calculated parameters of the third body enable us to determine the mass function $f_m(M_\odot)$ of the triple system. By assuming a coplanar orbit ($i = 90°$), we obtained the lower limit for the mass of the third component. The derived parameters of the LTTE solution are listed in Table 4 and the resulting curve for the third-body effect is plotted in the right panel of Figure 6. By considering the estimated mass of the third body, a brown dwarf is possible.

In the following, we apply Period04 (Lenz & Breger 2005) to the residuals of the LTTE. The periodogram is plotted in Figure 7. The highest peak in the periodogram has a period of 0.8566 d.

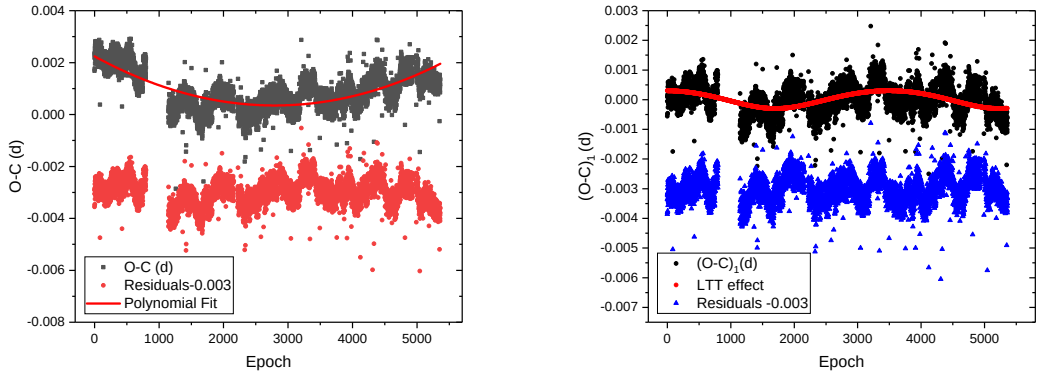

Fig. 6 *Left panel*: fitting the quadratic function to the $O-C$ curve of the primary minima; $O-C$ curve of the primary minima (*black squares*), quadratic function fit (*solid red line*) and residuals of this fitting (*red circles*). *Right panel*: LTTE on the residuals of quadratic fit; residuals of quadratic fit (*black squares*), LTTE (*red circles*) and residuals of LTTE (*blue triangles*).

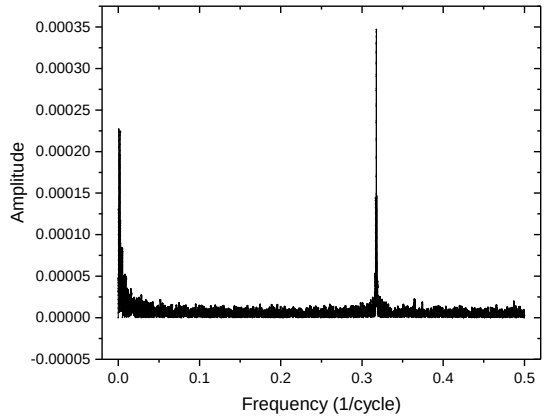

Fig. 7 Periodogram of residuals after removing the LTTE.

Table 4 Parameters of the Third Body around KIC 9026766

Parameter	Value for the Third Body
Eccentricity (e)	0.2 ± 0.005
Omega (ω)	259.2 ± 1.8
A (the semi-amplitude) (d)	$3.0E-4 \pm 1.5E-4$
T_0	2456372.0000
Projected semi-major axis $a_{1,2}\sin(i)$(au)	$5.197E-2 \pm 2.598E-2$
Mass Function, $f_m(M_\odot)$	$1.98E-5 \pm 0.9E-9$
Period of the third body (d)	972.5866 ± 0.0041
$M_3\sin(i)(M_\odot, i=90)$	0.029

Thus, we calculated the relative luminosity of the primary and secondary eclipses (Min I − Min II) for every light curve over 4 yr. The peak frequency is $f = 1.16738 \pm 9.8133e-6(\frac{1}{d})$, which is equal to a period of 0.8566 d (see the left panel of Fig. 8). In the right panel of Figure 8, the light curve for 2 d is plotted and red arrows mark when the depth of the primary minima is less than that of the secondary ones. This occurs almost every 0.8566 d, so the reason for this short periodicity is the exchange between the primary and secondary minima, which affects the $O-C$ curve of minima.

Another possible reason for the cyclic variations in the $O-C$ curve of minima is the Applegate effect. The magnetic field of stars could produce angular momentum transfer among its internal and external layers, causing orbital period changes (Applegate 1992).

$$\frac{\Delta(P)}{P} = 2\pi \frac{(O-C)}{P_{mod}} \tag{5}$$

where $(O-C)$ is the amplitude of the $O-C$ curve and P_{mod} is the luminosity period changes. Having the same period as the $O-C$ period modulation is necessary. To calculate the luminosity period changes, we considered the flux in the first and second maxima of individual light curves over 4 yr. Then, we calculated the period modulation for the difference in the primary and secondary maxima; $P_{mod} = 0.8566$ d, so $\frac{\Delta(P)}{P} \approx 2.538 \times 10^{-3}$. This short periodic oscillation and the value of $\frac{\Delta(P)}{P}$ suggest that the Applegate mechanism cannot explain the cyclic variations in the $O-C$ curve.

As mentioned in Section 2, the two nearby stars located within 0.5 and 1 arcsec of our target can cause background effects, which may not be noticed in the pixel data. This can cause a signal with a period of just more than three times the orbital period. The spot evolution in contact binaries can affect the eclipse times and mimic changes in the orbital period (Tran et al. 2013). In the following, we consider the spot evolution as the main reason for changes in the $O-C$ curves of minima.

To examine the effect of spots on the $O-C$ curve of minima, we utilized the theoretical formula derived

Table 5 Remaining Frequency Peaks in $O-C$ Curve

Frequency (1/cycle)	Amplitude (d)	Period (d)
$f_1 = 0.0020518 \pm 3.06486e-6$	$0.0002258 \pm 6.610e-6$	132.6288 ± 0.1982
$f_2 = 0.0007368 \pm 3.06486e-6$	$0.0002216 \pm 6.610e-6$	369.3374 ± 1.5333
$f_3 = 0.001679 \pm 3.37546e-6$	$0.0001782 \pm 6.610e-6$	169.0733 ± 0.3257
$f_4 = 0.001380 \pm 3.7932e-6$	$0.0001626 \pm 6.610e-6$	197.1940 ± 0.5410

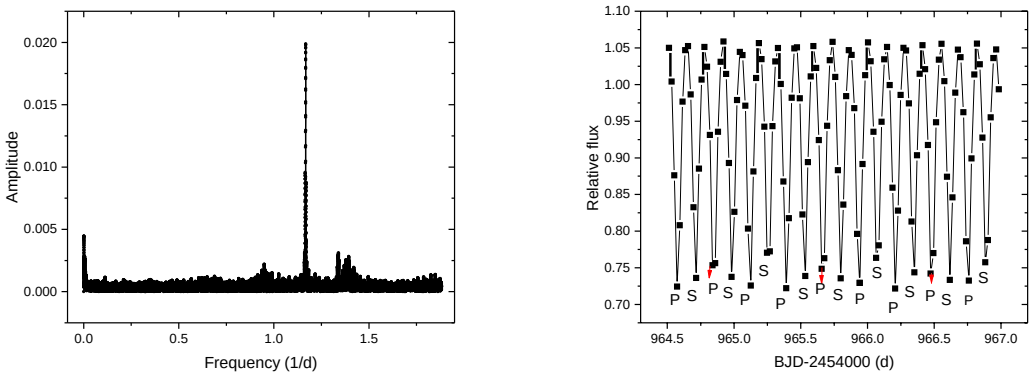

Fig. 8 *Left panel*: periodogram of the relative luminosity of the primary and secondary eclipses (Min I − Min II). *Right panel*: light curve over two days; primary minima are denoted by P and secondary ones by S; *red arrows* mark when the depth of the primary minima is less than that of the secondary ones.

by Pribulla et al. (2012) to estimate the amplitude (~ 0.0004 d) of eclipse timing variations, which are sorted by the remaining frequency peaks (which remain after removing the third-body peak) in the periodogram of the $O-C$ curve (see Table 5). Additionally, the observed quasi-periods of 132–200 d are in good agreement with periods of 50–200 d that were observed for contact binaries in the Kepler field of view (Tran et al. 2013). The remaining frequency peaks in the periodogram of the $O-C$ curve are listed in Table 5.

6 DISCUSSION AND CONCLUSION

We studied a short-period W UMa binary, KIC 9026766, in the Kepler field of view. Our study had two parts. In the first part, we derived the fundamental stellar parameters of the light curve using PHOEBE Legacy. For this purpose, we performed an automated q-search and found the mass ratio of the binary ($q = 2.077 \pm 0.0068$). We assumed the more massive is a main sequence and according to the spectral type K2, the estimated mass is $M_2 = 0.73\,M_\odot$ (Cox 2000). The mass of the primary component is calculated as $M_1 = 0.35\,M_\odot$. Our solution confirmed that KIC 9026766 is a near-contact binary with a fill-out factor of 0.2 percent.

In the second part, we studied the $O-C$ curves of minima to investigate the orbital variation. This target is flagged as TM on the Kepler website, so it was feasible to investigate the presence of a third body. By fitting a quadratic function to the $O-C$ curve of the primary minima, we calculated a period variation of $\dot{P} = 1.784911 \times 10^{-9} \pm 7.08752 \times 10^{-12}$ d yr^{-1}. Moreover, we inferred there is a third body with a period of 972.5866 ± 0.0041 d and a mass of $M = 0.029\,M_\odot$.

The modulation periods for the difference between the maxima and the main peak of periodogram analysis of residuals of the third-body effect as well as the observed frequency peak for the relative luminosity of the primary and secondary eclipses have the same values. The Applegate mechanism and spot motion cannot explain the existence of this signal with a period of just more than three times the orbital period. Background effects are possible because of the two nearby stars Gaia DR2 2127972818460821504 and Gaia DR2 212 7972818467257344. For the rest of the signals in the periodogram of the $O-C$ curve of minima, spot evolution was considered and the values of the amplitude and periods of the signals implied the effect of spot motion on the system components.

Acknowledgements The authors would like to thank Kyle Conroy for helpful discussions. This paper has made use of data from the Kepler mission. Funding for the Kepler mission is provided by the NASA Science Mission directorate. This research has made use of SIMBAD and VIZIER databases, operated at CDS, Strasbourg, France.

This research has made use of Lightkurve, a Python package for Kepler and TESS data analysis.

References

Abdul-Masih, M., Prša, A., Conroy, K., et al. 2016, AJ, 151, 101
Applegate, J. H. 1992, ApJ, 385, 621
Balaji, B., Croll, B., et al. 2015, MNRAS, 448, 429
Borkovits, T., Hajdu, T., Sztakovics, J., et al. 2016, MNRAS, 455, 4136
Borkovits, T., & Hegedüs, T. 1996, A&AS, 120, 63
Borkovits, T., Rappaport, S., et al. 2015, MNRAS, 448, 946
Conroy, K. E., et al. 2018, ApJ, 854, 163
Conroy, K. E., Prša, A., Stassun, K. G., et al. 2014, AJ, 147, 45
Cox, A. N. 2000, Allens Astrophysical Quantities (New York: Springer)
Lightkurve Collaboration et al. 2018, Astrophysics Source Code Library (ascl: 1812.013)
Guinan, E. F., & Maloney, F. P. 1985, AJ, 90, 1519
Hilditch, R. W. 2001, An Introduction to Close Binary Stars (Cambrige Univ. Press)
Irwin, J. B. 1952, ApJ, 116, 211
Lenz, P., & Breger, M. 2005, Communications in Asteroseismology, 146, 53
Lucy, L. B. 1967, Zeitschrift fur Astrophysik, 65, 89
Matijevič, G., Prša, A., et al. 2012, AJ, 143, 123
Pietrzyński, G., Graczyk, D., Gallenne, A., et al. 2019, Nature, 567, 200
Pribulla, T., Chochol, D., Tremko, J., et al. 2000, Contributions of the Astronomical Observatory Skalnate Pleso, 30, 117
Pribulla, T., Vaňko, M., Ammler-von Eiff, M., et al. 2012, Astronomische Nachrichten, 333, 754
Prša, A., Batalha, N., Slawson, R. W., et al. 2011, AJ, 141, 83
Rucinski, S. M. 1969, Acta Astronomica, 19, 245
Shklovskii, I. S. 1970, Soviet Ast., 13, 562
Skrutskie, M. F., Cutri, R. M., Stiening, R., et al. 2006, AJ, 131, 1163
Soomandar, S., & Abedi, A. 2020, New Astron., 80, 101394
Torres,, G., Vaz L. P. R., et al. 2014, AJ, 147, 36
Tran, K., Levine, A., Rappaport, S., Borkovits, T., et al. 2013, ApJ, 774, 81
van Hamme, W. 1993, AJ, 106, 2096